AGU PUBLICATIONS

Geophysical Research Letters

RESEARCH LETTER
10.1002/2015GL064912

Key Points:
- Only three-dimensional GCM simulations produce asymmetry in surface methane
- Eddies transport moisture away from poles into cross-equatorial Hadley circulation
- Eddies are asymmetric and therefore produce net northward transport of methane

Correspondence to:
J. M. Lora,
jlora@ucla.edu

Citation:
Lora, J. M., and J. L. Mitchell (2015), Titan's asymmetric lake distribution mediated by methane transport due to atmospheric eddies, *Geophys. Res. Lett.*, *42*, 6213–6220, doi:10.1002/2015GL064912.

Received 11 JUN 2015
Accepted 24 JUL 2015
Accepted article online 31 JUL 2015
Published online 14 AUG 2015

Titan's asymmetric lake distribution mediated by methane transport due to atmospheric eddies

Juan M. Lora[1] and Jonathan L. Mitchell[1,2]

[1]Department of Earth, Planetary, and Space Sciences, University of Calilfornia, Los Angeles, California, USA, [2]Department of Atmospheric and Oceanic Sciences, University of Calilfornia, Los Angeles, California, USA

Abstract The hemispheric asymmetry of Titan's surface methane has been proposed to be a consequence of orbital forcing affecting Titan's hydrologic cycle, but the mechanism behind asymmetrical transport of moisture remains to be examined. Using general circulation model simulations of Titan's atmosphere, we show that atmospheric moisture transport by three-dimensional tropospheric eddies is critical in generating Titan's surface liquid asymmetry. Comparison of axisymmetric and three-dimensional simulations demonstrates that a significant asymmetry only develops in the latter case. Analysis of the components of the three-dimensional moisture transport reveals that nonaxisymmetric eddies transport methane away from the poles and into the midlatitudes, where they transfer moisture into the cross-equatorial transport by the mean meridional circulation, producing an atmospheric "bucket brigade." Because these high-latitude, baroclinic eddies are more intense in the south than in the north, the net transport is preferentially northward, with the northern hemisphere gaining surface liquid at the expense of the southern hemisphere.

1. Introduction

Saturn's moon Titan supports a significant reservoir of liquid on its surface, primarily composed of methane [e.g., *Mastrogiuseppe et al.*, 2014]. One of the more striking aspects of this methane reservoir is the dramatic asymmetry of its distribution [*Aharonson et al.*, 2009]. Titan's north polar surface is covered with large seas and numerous lakes [*Stofan et al.*, 2007; *Hayes et al.*, 2008], while Ontario Lacus [*Turtle et al.*, 2009] is the only significant body of liquid in the southern hemisphere. This hemispheric asymmetry has been proposed to be a consequence of orbital forcing affecting Titan's hydrologic cycle, since the southern hemisphere currently undergoes a shorter but more intense summer than the north as a result of Saturn's orbital eccentricity of 0.054 [*Aharonson et al.*, 2009], but the mechanism that accomplishes this has not been clearly identified.

General circulation models (GCMs) of Titan have shown that surface methane efficiently evaporates from equatorial regions and builds up at higher latitudes [*Rannou et al.*, 2006; *Mitchell et al.*, 2006; *Mitchell*, 2008; *Schneider et al.*, 2012; *Lora et al.*, 2015] as a result of the atmospheric circulation, in agreement with observations of largely arid low latitudes [*Lorenz et al.*, 2006; *Radebaugh et al.*, 2008], wet polar regions [*Stofan et al.*, 2007; *Hayes et al.*, 2008; *Turtle et al.*, 2009], and significant convective cloud activity over the south pole during its summer [*Schaller et al.*, 2006; *Rodriguez et al.*, 2009; *Brown et al.*, 2010; *Turtle et al.*, 2011]. Moreover, recent Titan GCMs indicate that Saturn's current orbital configuration induces preferential surface liquid buildup in the north [*Schneider et al.*, 2012; *Lora et al.*, 2014]. As a consequence of more intense summers, the southern hemisphere may experience net evaporation [*Aharonson et al.*, 2009], or the northern hemisphere may receive higher precipitation due to its longer summers [*Schneider et al.*, 2012]. We demonstrate below that the orbital forcing results in a net northward transport of methane by the atmosphere, responsible for driving the observed asymmetry.

A primary motivation for this study is that axisymmetric (henceforth 2-D) GCMs of Titan fail to produce any significant latitudinal asymmetry in the surface liquid reservoir [i.e., *Mitchell*, 2008], in contrast to the fully three-dimensional (henceforth 3-D) models [*Schneider et al.*, 2012; *Lora et al.*, 2014] that resolve atmospheric eddies. This hints at the importance of three-dimensional dynamics in transporting methane. On Earth, net moisture transport by the atmosphere is the sum of transport by the mean meridional circulation and eddies [e.g., *Trenberth and Stepaniak*, 2003], with the latter being globally poleward and dominated by eastward propagating baroclinic waves in the subtropics and midlatitudes [*Peixoto and Oort*, 1992;

Shaw and Pauluis, 2012]. To self-consistently explore the components of moisture transport in Titan's atmosphere, we investigate 2-D and 3-D simulations of Titan's climate using the same modeling framework. We employ the Titan Atmospheric Model (TAM) [*Lora et al.*, 2015] to perform this comparison and examine the partitioning of moisture transport responsible for generating the observed asymmetry.

2. Model and Simulations

TAM is a three-dimensional GCM for Titan, based on the Geophysical Fluid Dynamics Laboratory spectral dynamical core [*Gordon and Stern*, 1982], which includes fully nongray radiative transfer as well as parameterizations of evaporation, condensation, precipitation, and hydrology to simulate Titan's methane hydrologic cycle, and has been shown to realistically simulate many features of Titan's atmosphere [*Lora et al.*, 2015]. In order to properly isolate the effects of the three-dimensional circulation, we run TAM under diurnal mean and full diurnal cycle insolation distributions to simulate 2-D and 3-D circulations, respectively, with all other boundary conditions kept identical. (In the absence of nonaxisymmetric forcing, boundary, or initialization conditions, the circulation remains axisymmetric even in a three-dimensional model. Similar 2-D to 3-D comparisons have been undertaken for Earth's circulation [e.g., *Becker et al.*, 1997].) In both cases we use a 32-layer (L32) atmosphere at T42 resolution, initialized from an axisymmetrized steady state from previous results [*Lora et al.*, 2015], with the initial surface liquid distribution replaced by 100 m reservoirs poleward of 60° in both hemispheres and dry land elsewhere, to approximate the observed liquid distribution in an idealized fashion that still maintains both zonal and latitudinal symmetry. We intentionally avoid an initially asymmetric distribution. Note that our adopted distribution can be interpreted as including possible "wetlands" at the lower elevation polar regions [*Neish and Lorenz*, 2014]. TAM's original bucket hydrology scheme is retained; in addition, we incorporate an idealized infiltration scheme at the lower latitudes, wherein surface liquid above a threshold 100 kg m^{-2} decreases at a slow constant rate, set to 1 mm per (Earth) day. This scheme is only active in the 3-D simulation, as no equatorial precipitation occurs in the 2-D case, consistent with equatorial convection being organized by three-dimensional, planetary-scale waves [*Mitchell et al.*, 2011].

Changes in surface liquid distributions after 10 Titan years of 2-D and 3-D simulations show important differences (Figure 1a). In the 2-D case, only a very small north-south asymmetry develops, which is dominated by the slight difference between the northern and southern hemispheres in the latitude (~73°N/S) where there is zero change in surface liquid. Elsewhere in the polar regions, surface liquid changes are approximately equal and occur at the same latitudes, showing that regions of net evaporation and net precipitation are essentially equal between the hemispheres. Overall, the patterns of drying and wetting in both hemispheres indicate that surface methane is transported about 10° poleward by the atmosphere without creating an asymmetry; net increases peak around 75° and decrease toward the poles.

In contrast, the 3-D simulation develops a clear hemispheric asymmetry: In this case, the liquid change in both hemispheres increases toward the poles, making the latitudinal distribution smoother, but the region of drying in the southern hemisphere is much more pronounced and extends considerably farther poleward than its northern counterpart. Conversely, the area of net surface accumulation (positive surface liquid change) extends several degrees of latitude farther equatorward in the north. Indeed, the total change in surface liquid methane (i.e., the integral of the curves in Figure 1a) is negative for the southern hemisphere and positive for the northern, indicating a northward pole-to-pole transport by the atmosphere of roughly 5×10^{14} kg of methane per Titan year. This comparison confirms that a three-dimensional atmospheric circulation is critical for the development of the observed surface liquid asymmetry, while the purely axisymmetric circulation can only move the surface liquid farther poleward in each hemisphere.

3. Moisture Transport and Atmospheric Eddies

We turn to an examination of the properties of the 3-D simulation that produce the asymmetric net transport. The study of moisture transport on Earth is well established [*Starr and Peixoto*, 1971; *Peixoto and Oort*, 1992], and we draw from that literature the approach of separating the atmospheric moisture transport into mean circulation and transient contributions from eddies. To examine the components of moisture transport by the atmosphere, simulated specific humidity and meridional wind at each grid cell, q and v, are resolved as follows:

$$q = \overline{q} + q', \tag{1}$$

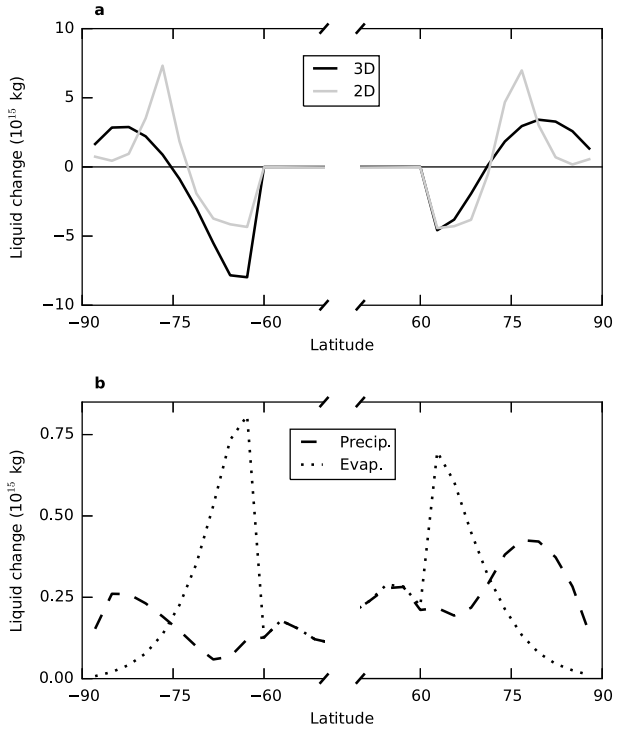

Figure 1. Simulated polar surface liquid changes and their asymmetries. (a) Differences in the total simulated surface liquid between the end of year 10 and the initial distributions for axisymmetric (2-D) and three-dimensional (3-D) simulations only display a distinct hemispheric asymmetry in the latter case, indicating net northward transport of methane. (b) Total precipitation and evaporation over the last year of the 3-D simulation indicate that asymmetries in both contribute to that of the surface liquid.

$$v = \overline{v} + v', \tag{2}$$

where overbars denote time averages, and primes deviations therefrom. Similarly,

$$q = [q] + q^*, \tag{3}$$

$$v = [v] + v^*, \tag{4}$$

where the square brackets denote zonal averages, and asterisks deviations therefrom. Using equations (1)–(4), time and zonal mean meridional fluxes are

$$[\overline{qv}] = [\overline{q}][\overline{v}] + \left[\overline{q'v'}\right] + \left[\overline{q}^*\overline{v}^*\right], \tag{5}$$

where the terms on the right-hand side represent, respectively, transport by the mean meridional circulation, transient perturbations, and stationary eddies. In contrast to moisture transport on Earth [*Trenberth and Stepaniak*, 2003], the stationary eddy term is negligible in our simulations since we exclude any continuously asymmetric forcing (only the instantaneous diurnal forcing, in the 3-D simulation, is zonally asymmetric). Finally, the vertically integrated meridional moisture transport is

$$F = \frac{1}{g}\int_{p_s}^{0} qv \, \mathrm{d}p, \tag{6}$$

where p and p_s are pressure and its surface value, and g is acceleration due to gravity. All components of moisture transport presented are similarly vertically integrated.

A comparison of the moisture transport terms from the final year of the simulations is shown in Figure 2. In both simulations, total moisture transport (Figures 2a and 2b) is strongly seasonal, as a result of Titan's reversing cross-equatorial circulation. The circulation transports methane into the summer hemisphere, opposite its overall energy flux [*Mitchell*, 2012; *Lora et al.*, 2014]; moisture fluxes are therefore globally southward during southern spring and summer, and northward during northern spring and summer. Moisture transport is considerably more vigorous in the 3-D case. Furthermore, the annual mean, which is largely a cancelation of the two seasonal phases, shows net northward transport in the 3-D case, in contrast to the 2-D simulation. The moisture flux is entirely northward between 60°N and 90°N, and southward only poleward of ~70°S, consistent with some methane from the surface reservoir between 60°S and 70°S being transported to the north by the atmosphere.

Transport in the 3-D simulation by the mean meridional circulation (Figure 2c) also varies seasonally, corresponding to the presence and seasonal reversal of Titan's tropospheric Hadley circulation. This component is the dominant mode of moisture transport at lower and middle latitudes and is also responsible for the seasonal reversal of the total moisture flux direction. The annual mean moisture transport is asymmetric, with low-latitude transport dominated by northward flux between 45°S and 10°N and poleward transport into the southern pole significantly stronger than in the north.

Moisture fluxes due to transient perturbations (Figure 2d) largely compensate those by the mean meridional circulation, but also conspicuously lack a seasonal cycle. At lower latitudes, roughly between ~40°S and 40°N, this transport is small and nearly symmetric about the equator. Poleward of these latitudes, however, it is of comparable magnitude to transport by the mean circulation, and acts to move methane *out* of regions with

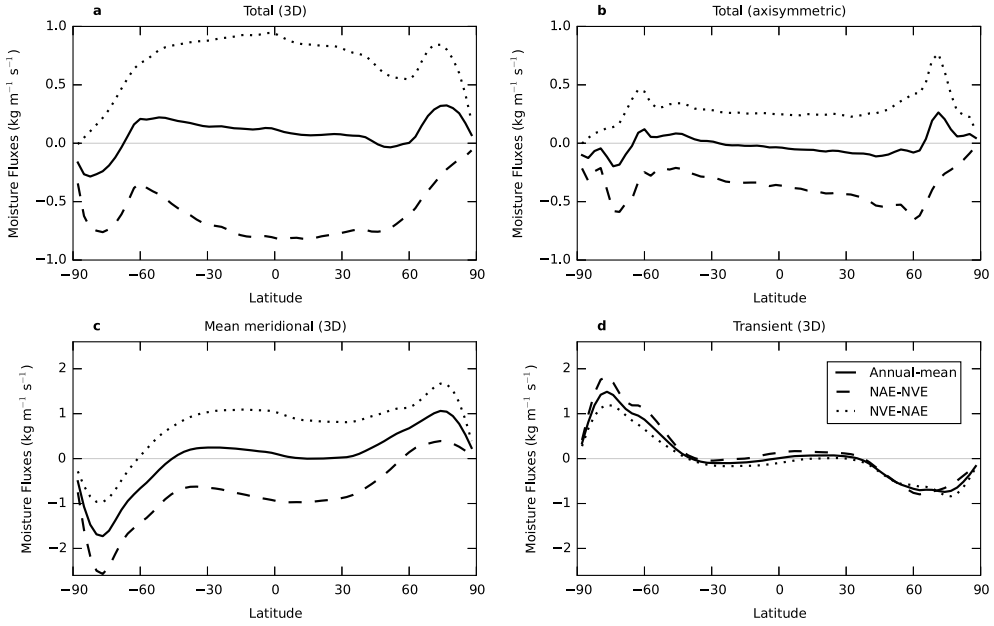

Figure 2. Simulated meridional moisture fluxes: Total zonal mean meridional moisture fluxes from (a) the three-dimensional (3-D) simulation and (b) the axisymmetric (2-D) simulation. The total moisture flux in the 3-D case is made up of (c) strongly seasonal transport due to the mean meridional circulation and (d) largely constant transport, strong at high latitudes, due to transient perturbations, which are generally opposite in direction. The legend for all panels is in Figure 2d; NAE and NVE correspond to northern autumnal and vernal equinox, respectively, so that NAE−NVE is northern autumn and winter, and NVE−NAE is northern spring and summer.

surface liquid, i.e., equatorward. The vast majority of moisture transport by transient perturbations in the 3-D simulation is due to transport by nonaxisymmetric eddies (Figure 3a), which in the annual mean is nearly identical to that due to transients. In other words, three-dimensional eddies, which are both nonaxisymmetric and transient, produce the equatorward moisture transport that occurs at high latitudes (Figure 2d), which is opposite in direction to its equivalent in Earth's atmosphere.

In the summer hemisphere, eddies counteract the poleward moisture transport due to the mean circulation, and in the winter hemisphere further transport moisture into the midlatitudes. Transport by the mean meridional circulation is never northward over the southern pole where surface liquids reside (Figure 2c), so the net northward methane transport is directly attributable to eddies. The combined winter hemisphere moisture transport resembles a "bucket brigade": eddies transport methane out of the polar region and transfer the moisture to the cross-equatorial Hadley cell. Furthermore, the peak fluxes due to transients are approximately

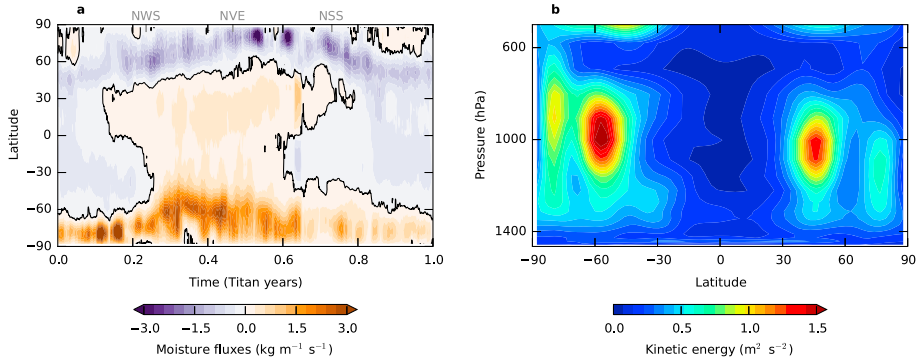

Figure 3. Moisture transport by asymmetric eddies. Meridional moisture fluxes (a) for nonaxisymmetric components, i.e., $[q^*v^*]$, for the last year of the 3-D simulation. (b) Annual and zonal mean eddy kinetic energy in the troposphere, showing a considerable asymmetry between hemispheres. Both panels exhibit strong polar activity, particularly in the south. Black line in Figure 3a corresponds to contour of zero transport. Northern winter solstice (NWS), vernal equinox (NVE), and summer solstice (NSS) are labeled at the top.

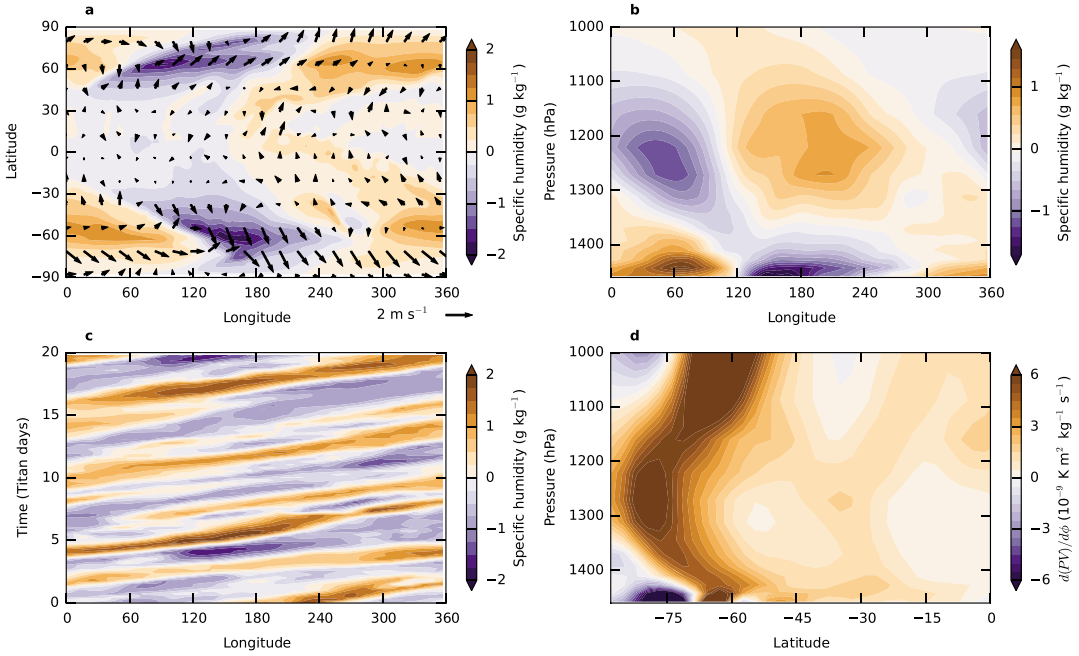

Figure 4. Titan's transient tropospheric eddies. Snapshots of (a) surface level specific humidity anomalies (q^*) and winds and (b) specific humidity anomalies at 60°S shortly after northern vernal equinox show clear nonaxisymmetric features (Figure 4a) and westward tilts in the vertical (Figure 4b). (c) The evolution of low-level specific humidity anomalies at 60°S after northern vernal equinox shows the eddies propagate eastward at 1–2 m s^{-1}. (d) Latitudinal gradients of zonal mean potential vorticity (d PV/dϕ) for the same time period show marked reversals in the vertical direction, indicative of baroclinic instability.

twice as strong in the south as in the north, leading to stronger blocking of summertime poleward moisture transport by the Hadley cell, as well as increased wintertime transport out of high latitudes. As a result, in the annual mean, the eddies asymmetrically feed moisture to the cross-equatorial mean meridional circulation, preferentially in the southern hemisphere. In response, transport due to the mean meridional circulation is also hemispherically asymmetric, and the net result is northward methane moisture transport.

The low seasonality of transport due to the transient eddies is illustrated in Figure 3a. At low latitudes, the directionality of this transport reverses with season and is also opposite to the moisture transport by the mean meridional circulation (as in Earth's tropics [*Trenberth and Stepaniak*, 2003]), but in those regions it is comparatively unimportant (cf. Figures 2c and 2d) and hemispherically symmetric. At higher latitudes, most of the seasonality manifests as shifts in the latitudes of maximum equatorward transport; in both hemispheres, these maxima shift equatorward around summer solstice and slowly migrate back poleward over the subsequent seasons. In the northern pole during its summer and autumn, there is a region of poleward moisture transport by transient eddies that is responsible for the flattening of the transport in Figure 2d at these latitudes. There is only a hint of similar summertime poleward transport in the south, and as a result the net equatorward transport due to transients is close to twice as high in the south as in the north. This stark difference is responsible for the asymmetric net total transport of moisture by the eddies.

A further examination of eddy activity shows that eddies in Titan's atmosphere respond nonlinearly to Titan's seasonal forcing: Figure 3b shows the annual mean eddy kinetic energy (defined as $(u^{*2}+v^{*2})/2$, where u^* and v^* are the deviations from zonal means of zonal and meridional wind components, respectively). Throughout the atmosphere and, in particular, in the middle to lower troposphere where the majority of moisture transport takes place, the annual mean eddy kinetic energy is latitudinally asymmetric, with higher energies in a larger region in the southern hemisphere. Notably, the local eddy kinetic energy peak at midlatitudes is strong closer to the surface and shifted significantly poleward in the south compared to the north and as a result occurs closer to the surface liquid source in that hemisphere.

Figures 4a and 4b show snapshots of horizontal and vertical cross sections of eddies around northern vernal equinox. Significant near-surface specific humidity perturbations of zonal wave numbers 1 to 2 extend

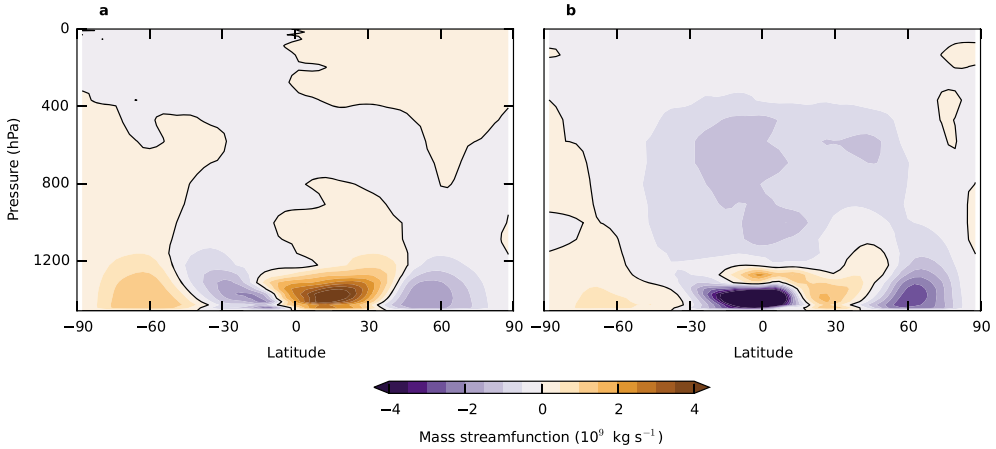

Figure 5. Simulated mass stream functions. (a) Annual mean mass stream function from the last year of the 3-D simulation, showing Hadley cells (low to middle latitudes) and eddy-driven "Ferrel cells" (middle to high latitudes) in the lower troposphere. (b) As in Figure 5a but showing the stream function for the 500 Earth days bracketing northern summer solstice. Positive values indicate clockwise circulation; the black contour shows the zero streamline.

between poles and midlatitudes, where moisture transport is dominated by eddies. These perturbations also display a significant westward tilt in the vertical direction between the surface and roughly 1000 hPa, which is characteristic of baroclinic disturbances and associated with extratropical cyclones on Earth. The eddies propagate eastward (Figure 4c) with speeds of 1–2 m s^{-1}, which are comparable to the background zonal wind at their location and therefore indicative of slow relative phase speeds, also compatible with baroclinic waves similar to those responsible for poleward moisture transport in Earth's midlatitudes [*Trenberth and Stepaniak*, 2003; *Shaw and Pauluis*, 2012]. The presence of baroclinic instabilities can be substantiated by sign changes in the vertical direction of the latitudinal gradient of potential vorticity (akin to the Rayleigh-Kuo criterion [*Vallis*, 2006]). Such reversals are indeed apparent at low altitudes and high latitudes (Figure 4d) in the 3-D simulation, confirming the presence of shallow baroclinic eddies.

Eddy activity in the low troposphere is also discernible in the meridional mass stream function (Figure 5), wherein the thermally direct Hadley circulation is flanked by thermally indirect cells between midlatitudes and the poles, resembling Earth's low-latitude and midlatitude circulation. These cells must be eddy driven, implying eddy fluxes of quantities other than moisture. In the annual mean, a hemispheric asymmetry is also visible in these cells, which appear "shifted" to the south, similarly to the eddy kinetic energies. A strong circulation is particularly apparent below 1200 hPa, where the eddy cells are dominant, consistent with shallow baroclinic eddies and a seasonal layer capped by the stability of the free troposphere [*Charnay and Lebonnois*, 2012]. In the upper troposphere and stratosphere, the circulation is dominated by thermally direct cells.

4. Discussion and Conclusions

Orbital influences (i.e., due to seasonal differences) on Titan's hydrologic cycle require a nonlinear mechanism to produce Titan's asymmetric surface liquid distribution since, in the annual mean, the insolation distribution is hemispherically symmetric [*Aharonson et al.*, 2009]. Transport due to three-dimensional transient eddies in Titan's atmosphere, which we have shown is strongly asymmetric in the annual mean, provides such a mechanism. Though the liquid distribution from our 2-D simulation is not perfectly symmetric about the equator, the eddies produced in the 3-D simulation dramatically increase the north-south differences in moisture transport and, in turn, the evolution of surface liquids (Figure 1). The interaction of equatorward transport by tropospheric baroclinic eddies and the cross-equatorial mean meridional circulation produces a total meridional moisture transport that is mostly northward in the annual mean, definitively moving methane from southern to northern hemispheres, and wetting the latter at the expense of the former (in the present orbital configuration [*Lora et al.*, 2014]).

The net pole-to-pole transport of methane in our 3-D simulation suggests a timescale of 10^3–10^4 (Earth) years to move the surface reservoir between poles, assuming a total volume of liquid of $\sim 10^5$ km^3 [*Lorenz et al.*, 2008; *Mastrogiuseppe et al.*, 2014]. The timescale may be considerably longer since the area of contact

between surface liquids and the atmosphere is smaller on Titan than in our simulations. Nevertheless, our estimate provides a lower bound, which is sufficiently short to allow a significant response to orbital changes with periods of 10^4–10^5 years [*Lora et al.*, 2014; *Aharonson et al.*, 2009].

On Titan, the liquid distribution is not zonally symmetric nor is the possible extent of potential wetlands necessarily symmetric about the equator. In addition to localized lakes and seas, Titan has surface topography [*Lorenz et al.*, 2013] that likely affects the circulation of the lower troposphere [*Tokano*, 2008] and is ignored in our study. As such, our simulations represent an idealized scenario employed specifically to isolate asymmetric dynamical mechanisms in the atmosphere. Our implementation of the surface liquid distribution produces strong surface temperature gradients near the transition zones from dry land to liquid (60°N/S) via evaporative cooling. The resulting temperatures of the lower troposphere, which are affected by the surface, therefore have zones of relatively strong gradients that are sources of baroclinicity, which may artificially increase eddy activity. Nevertheless, the surface temperature distribution from the 3-D simulation is very similar to the zonal mean distribution from previous TAM simulations that included representations of individual lakes and seas [*Lora et al.*, 2015], suggesting that the impact of our assumptions here is not unphysical. In reality, while temperature gradients will likely be more complicated in distribution, the presence of surface methane on Titan and Titan's observed surface temperatures [*Jennings et al.*, 2011] suggest that similar baroclinicity may be possible, at least locally if not in a zonally coherent distribution. Moreover, low-level baroclinic waves were also identified in the *dry* GCM of *Lebonnois et al.* [2012], further corroborating their existence on Titan. Similarly, it is possible that stationary eddies on Titan play a nonnegligible role in the transport of moisture, as they do on Earth, which we have not investigated. It is not immediately obvious if such transport would be preferentially poleward or equatorward, so it could either amplify or dampen the effect that we describe.

In summary, by comparing 2-D and 3-D simulations of Titan's atmospheric circulation, we have shown that three-dimensional transient eddies in Titan's troposphere, dominant at high latitudes, play a critical role in generating the observed north-south asymmetry of Titan's surface liquids. The eddies respond nonlinearly to the solar heating of Titan's atmosphere and transport polar methane into Titan's cross-equatorial Hadley circulation. They therefore mediate the net northward atmospheric methane transport, providing a mechanism for the atmosphere-surface system to respond to Titan's Milankovitch cycles. Nonaxisymmetric eddy transport of momentum (and trace constituents) from three-dimensional waves in Titan's stratosphere has been the focus of previous study [*Hourdin et al.*, 1995; *Luz et al.*, 2003; *Newman et al.*, 2011; *Lebonnois et al.*, 2012] and is crucial for the development of Titan's characteristic superrotation. Our simulations demonstrate that a similar transport of methane, essential to Titan's hydrologic cycle, operates in Titan's troposphere, where three-dimensional planetary waves were already known to organize large outbursts of equatorial precipitation during equinoxes [*Mitchell et al.*, 2011].

Acknowledgments
This work was supported by NASA grants NNX12AI71G and NNX12AM81G. Data presented in this paper are available from the authors upon request.

The Editor thanks Benjamin Charnay and an anonymous reviewer for their assistance in evaluating this paper.

References

Aharonson, O., A. G. Hayes, J. I. Lunine, R. D. Lorenz, M. D. Allison, and C. Elachi (2009), An asymmetric distribution of lakes on Titan as a possible consequence of orbital forcing, *Nat. Geosci.*, *2*, 851–854.

Becker, E., G. Schmitz, and R. Geprägs (1997), The feedback of midlatitude waves onto the Hadley cell in a simple general circulation model, *Tellus, Ser. A*, *49*, 182–199.

Brown, M. E., J. E. Roberts, and E. L. Schaller (2010), Clouds on Titan during the Cassini prime mission: A complete analysis of the VIMS data, *Icarus*, *205*, 571–580.

Charnay, B., and S. Lebonnois (2012), Two boundary layers in Titan's lower troposphere inferred from a climate model, *Nat. Geosci.*, *5*(2), 106–109.

Gordon, C. T., and W. F. Stern (1982), A description of the GFDL global spectral model, *Mon. Weather Rev.*, *110*, 625–644.

Hayes, A., et al. (2008), Hydrocarbon lakes on Titan: Distribution and interaction with a porous regolith, *Geophys. Res. Lett.*, *35*, L09204, doi:10.1029/2008GL033409.

Hourdin, F., O. Talagrand, R. Sadourny, R. Courtin, D. Gautier, and C. P. McKay (1995), Numerical simulations of the general circulation of the atmosphere of Titan, *Icarus*, *117*, 358–374.

Jennings, D., et al. (2011), Seasonal changes in Titan's surface temperatures, *Astrophys. J.*, *737*(1), L15.

Lebonnois, S., J. Burgalat, P. Rannou, and B. Charnay (2012), Titan global climate model: A new 3-dimensional version of the IPSL Titan GCM, *Icarus*, *218*, 707–722.

Lora, J. M., J. I. Lunine, J. L. Russell, and A. G. Hayes (2014), Simulations of Titan's paleoclimate, *Icarus*, *243*, 264–273.

Lora, J. M., J. I. Lunine, and J. L. Russell (2015), GCM simulations of Titan's middle and lower atmosphere and comparison to observations, *Icarus*, *250*, 516–528.

Lorenz, R. D., et al. (2006), The sand seas of Titan: Cassini RADAR observations of longitudinal dunes, *Science*, *312*, 724–727.

Lorenz, R. D., et al. (2008), Titan's inventory of organic surface materials, *Geophys. Res. Lett.*, *35*, L02206, doi:10.1029/2007GL032118.

Lorenz, R. D., et al. (2013), A global topographic map of Titan, *Icarus*, *225*, 367–377.

Luz, D., F. Hourdin, P. Rannou, and S. Lebonnois (2003), Latitudinal transport by barotropic waves in Titan's stratosphere. II. Results from a coupled dynamics-microphysics-photochemistry GCM, *Icarus*, *166*, 343–358.

Mastrogiuseppe, M., et al. (2014), The bathymetry of a Titan sea, *Geophys. Res. Lett.*, *41*, 1432–1437, doi:10.1002/2013GL058618.

Mitchell, J. L. (2008), The drying of Titan's dunes: Titan's methane hydrology and its impact on atmospheric circulation, *J. Geophys. Res.*, *113*, E08015, doi:10.1029/2007JE003017.
Mitchell, J. L. (2012), Titan's transport-driven methane cycle, *Astrophys. J.*, *756*, L26.
Mitchell, J. L., R. T. Pierrehumbert, D. M. W. Frierson, and R. Caballero (2006), The dynamics behind Titan's methane clouds, *Proc. Natl. Acad. Sci.*, *103*, 18,421–18,426.
Mitchell, J. L., M. Ádámkovics, R. Caballero, and E. P. Turtle (2011), Locally enhanced precipitation organized by planetary-scale waves on Titan, *Nat. Geosci.*, *4*, 589–592.
Neish, C. D., and R. D. Lorenz (2014), Elevation distribution of Titan's craters suggests extensive wetlands, *Icarus*, *228*, 27–34.
Newman, C. E., C. Lee, Y. Lian, M. I. Richardson, and A. D. Toigo (2011), Stratospheric superrotation in the Titan WRF model, *Icarus*, *213*, 636–654.
Peixoto, J. P., and A. H. Oort (1992), *Physics of Climate*, Am. Inst. of Phys., New York.
Radebaugh, J., et al. (2008), Dunes on Titan observed by Cassini Radar, *Icarus*, *194*, 690–703.
Rannou, P., F. Montmessin, F. Hourdin, and S. Lebonnois (2006), The latitudinal distribution of clouds on Titan, *Science*, *311*, 201–205.
Rodriguez, S., et al. (2009), Global circulation as the main source of cloud activity on Titan, *Nature*, *459*, 678–682.
Schaller, E. L., M. E. Brown, H. G. Roe, and A. H. Bouchez (2006), A large cloud outburst at Titan's south pole, *Icarus*, *182*, 224–229.
Schneider, T., S. D. B. Graves, E. L. Schaller, and M. E. Brown (2012), Polar methane accumulation and rainstorms on Titan from simulations of the methane cycle, *Nature*, *481*, 58–61.
Shaw, T. A., and O. Pauluis (2012), Tropical and subtropical meridional latent heat transports by disturbances to the zonal mean and their role in the general circulation, *J. Atmos. Sci.*, *69*, 1872–1889.
Starr, V. P., and J. P. Peixoto (1971), Pole-to-pole eddy transport of water vapor in the atmosphere during the IGY, *Arch. Meteorol. Geophys. Bioklimatol. A*, *20*, 85–114.
Stofan, E. R., et al. (2007), The lakes of Titan, *Nature*, *445*, 61–64.
Tokano, T. (2008), Dune-forming winds on Titan and the influence of topography, *Icarus*, *194*, 243–262.
Trenberth, K., and D. Stepaniak (2003), Covariability of components of poleward atmospheric energy transports on seasonal and interannual timescales, *J. Clim.*, *16*(22), 3691–3705.
Turtle, E. P., J. E. Perry, A. S. McEwen, A. D. Del Genio, J. Barbara, R. A. West, D. D. Dawson, and C. C. Porco (2009), Cassini imaging of Titan's high-latitude lakes, clouds, and south-polar surface changes, *Geophys. Res. Lett.*, *36*, L02204, doi:10.1029/2008GL036186.
Turtle, E. P., A. D. Del Genio, J. M. Barbara, J. E. Perry, E. L. Schaller, A. S. McEwen, R. A. West, and T. L. Ray (2011), Seasonal changes in Titan's meteorology, *Geophys. Res. Lett.*, *38*, L03203, doi:10.1029/2010GL046266.
Vallis, G. K. (2006), *Atmospheric and Oceanic Fluid Dynamics*, Cambridge Univ. Press, Cambridge, U. K.